Quaternary Science Reviews 295 (2022) 107742

Contents lists available at ScienceDirect

Quaternary Science Reviews

journal homepage: www.elsevier.com/locate/quascirev

Recharge variability in Australia's southeast alpine region derived from cave monitoring and modern stalagmite $\delta^{18}O$ records

Carol V. Tadros [a, b, *], Monika Markowska [c, a], Pauline C. Treble [a, b], Andy Baker [b, a], Silvia Frisia [d], Lewis Adler [e], Russell N. Drysdale [f]

[a] ANSTO, Lucas Heights, NSW, 2234, Australia
[b] School of Biological, Earth and Environmental Sciences, UNSW Sydney, Sydney, NSW, 2052, Australia
[c] Climate Geochemistry Department, Max Planck Institute for Chemistry, 55128, Mainz, Germany
[d] School of Environmental and Life Science, University of Newcastle, Callaghan, NSW, 2308, Australia
[e] Bioanalytical Mass Spectrometry Facility, Mark Wainwright Analytical Centre, UNSW Sydney, Sydney, NSW, 2052, Australia
[f] School of Geography, Earth and Atmospheric Sciences, University of Melbourne, Parkville VIC, 3052, Australia

ARTICLE INFO

Article history:
Received 11 April 2022
Received in revised form
24 August 2022
Accepted 30 August 2022
Available online 27 September 2022

Handling Editor: Dr Mira Matthews

Keywords:
Paleoclimatology
Australian alpine region
Speleothems
Stable isotopes
Recharge

ABSTRACT

Oxygen isotopic ($\delta^{18}O$) variations in stalagmite records have the potential to provide new insights about past climates beyond the instrumental record. This paper presents the first high-resolution oxygen isotope time series of three coeval stalagmite records from the alpine region of south-eastern Australia covering the period 1922–2006 CE. We use extended surface and cave monitoring datasets, petrographic investigation, modelled recharge time series and farmed calcite precipitates to assess the controls on speleothem $\delta^{18}O$ and investigate the coherence between three records from Harrie Wood Cave. The drip water response to recent interannual rainfall variability shows that cave drip water Cl^-, $\delta^{18}O$ and drip rate display a clear response to an increase in rainfall recharge. It is demonstrated that stalagmites from the same drip sites also record variability in interannual recharge, where an increase in $\delta^{18}O$ values is observed with lower recharge, while a decrease in $\delta^{18}O$ values correspond to higher recharge amounts. The three stalagmite $\delta^{18}O$ records are in broad agreement, showing common responses to relatively higher recharge between 1945 and 1995 CE and the low recharge periods between 1937 and 1945 CE (World War II drought) and late 1996 to 2006 CE (beginning of the Millennium Drought). However, differences in the magnitude of the relative response of each stalagmite $\delta^{18}O$ record varies. Based on evidence from our cave monitoring study and farmed calcites, we conclude that the differences between the three stalagmite records is attributed to variability in the contribution of preferential flows during recharge events and the store reservoir volume supplying the drip site. When the $\delta^{18}O$ decreases in response to enhanced recharge, the speleothem $\delta^{13}C$ also decreases, and this is interpreted to reflect a soil respiration response to changes in soil moisture availability due to recharge. Hence, stalagmite $\delta^{18}O$ from the Australian alpine region can be applied to reconstruct periods of relatively higher and lower rainfall recharge and thus extend our knowledge of the timing and relative magnitude of droughts as well as past periods of higher recharge in this region.

1. Introduction

Variations in the oxygen isotope ratios ($\delta^{18}O$) within cave calcite deposits, or speleothems, are a well-established proxy for palaeoclimate reconstructions (McDermott, 2004; Lachniet, 2009). Speleothem $\delta^{18}O$ values have been extensively interpreted to infer past climate variables, including precipitation amount, surface air temperature, moisture source regions and rainout effects, as the $\delta^{18}O$ signature of rainfall is dependent on all these (Dansgaard, 1964; Rozanski et al., 1993; Gat, 1996; Tan, 2014; Wang et al., 2017). Yet, at most cave sites the speleothem $\delta^{18}O$ does not directly reflect the surface signal. Instead, it is the product of a number of processes which modify the infiltrating meteoric precipitation $\delta^{18}O$ value as it is transported through the soil, karst and cave (Lachniet, 2009). Flow paths through the karst have an important control on the $\delta^{18}O$ values of water feeding the drip site.

* Corresponding author. ANSTO, Lucas Heights, NSW, 2234, Australia.
E-mail address: carol.tadros@ansto.gov.au (C.V. Tadros).

https://doi.org/10.1016/j.quascirev.2022.107742
0277-3791/

Recharge water that is mixed and stored in the karst produces $\delta^{18}O$ values reflecting the long-term weighted mean $\delta^{18}O$ value of local precipitation. By contrast, recharge from conduit and fracture flow paths result in shorter residence times in the karst, with drip water $\delta^{18}O$ time series capturing intra-annual and inter-annual variability (Baker et al., 2019). Given that the climate, karst and cave processes can significantly influence the preserved signal, correct interpretation of speleothem $\delta^{18}O$ records hinges on an understanding of the controls on calcite oxygen isotope compositions at a specific cave site. As such, site-specific calibration of modern stalagmite $\delta^{18}O$ time series against available cave monitoring datasets (e.g., Feng et al., 2012; Genty et al., 2014; Tadros et al., 2016; Riechelmann et al., 2017; Zhang et al., 2020), analysis of multiple speleothem records from the same cave and covering the same time period (e.g., Hercman et al., 2020), and examining modern speleothem $\delta^{18}O$ records against instrumental climate observations (e.g., Mickler et al., 2004; Cruz et al., 2005; Mattey et al., 2008; Baker and Bradley, 2010; Jex et al., 2010; Fairchild and Baker, 2012; Moquet et al., 2016; Markowska et al., 2020; Scroxton et al., 2021) can provide context for interpreting pre-instrumental $\delta^{18}O$ variability in stalagmite records to ensure proxy fidelity.

The Australian Alpine region has experienced a significant decline in snow cover with large year-to-year variability (Green and Pickering, 2009) and a decrease by up to 24% in precipitation and an increase in the frequency of drought and severe storms has been forecasted (Hennessy et al., 2003). Further, recent observed trends have shown that since the mid-1990s southeast Australia has experienced a decline in cool-season (April–October) rainfall (e.g., Freund et al., 2017; Rauniyar and Power, 2020). These climate changes will have a direct impact on surface and groundwater flows from the alpine catchments to major rivers and streams in the Murray-Darling Basin, which is estimated to deliver A$9.6 billion per annum in economic benefits through its contribution to the agricultural and tourism industry and for hydroelectric power generation (Worboys, and Good, 2011).

High-resolution speleothem $\delta^{18}O$ records from Harrie Wood Cave, a well-monitored cave located in the Australian Alpine karst region, can provide reliable evidence to assess the extent and intensity of past climate variability over periods longer than the instrumental record. In order to gain this longer-term perspective, calibration of climate proxies are pivotal for reliable reconstructions of the climate history. Recently, using long-term empirical observations from Harrie Wood Cave, water-flow dynamics in the unsaturated zone were characterised (Markowska et al., 2015) and the hydrological response of drip water $\delta^{18}O$ values at three monitored drip sites (HW1, HW2 and HW3) to local precipitation was substantiated (Tadros et al., 2016). However, in the high-altitude regions of southeast Australia, no previous research has been conducted to examine whether empirical monitoring datasets can reveal key insights into the climate signal preserved by a stalagmite $\delta^{18}O$ record. Rainfall generating groundwater recharge, or the vertical drainage of water from the surface to the aquifer, at the local scale is influenced by the timing and magnitude of precipitation and rainfall recharge thresholds (Baker et al., 2021). Here, observational rainfall data and calculated precipitation recharge thresholds for the montane climate is used to quantify recharge estimates in Harrie Wood Cave (Baker et al., 2021), then verified against 10-years of in-cave measurements.

In this context, three chronologically constrained stalagmite $\delta^{18}O$ records from Harrie Wood Cave (HW–S1, HW-S2 and HW_38 b), covering the period from 1922 to 2006 CE, are presented. High-resolution, 10-year surface and cave monitoring datasets from Harrie Wood Cave (Tadros et al., 2016, 2019) are updated and presented in this paper, together with a new time series of modelled recharge and results from in-cave precipitation experiments, including farmed calcite precipitates and instantaneous precipitation experiments. The modern stalagmite records are examined using perspectives from these datasets with an aim to: constrain the causes of speleothem $\delta^{18}O$ variability, and understand differences in oxygen isotope values between multiple records over the same growth interval. This paper also evaluates the link with longer-term drying and wetting over the last 84 years of contemporaneous growth, to ensure palaeoclimatic information is correctly interpreted. This research is a priority to address the lack of high-resolution speleothem palaeoclimate records in the high-altitude regions of SE Australia, which are highly vulnerable to climate change (Neukom and Gergis, 2012; Dixon et al., 2017). The findings in this research paper will provide much-needed knowledge to progress the development of climate proxies and will bridge interpretations of past climate reconstructions from speleothem $\delta^{18}O$ records.

2. Materials and methods

2.1. Harrie Wood Cave setting

Harrie Wood Cave (35°44′ S, 148°30′ E; Fig. 1) is located within the Yarrangobilly karst area, one of seven karst areas within Kosciuszko National Park which developed in Late Silurian (Ludlovian-age) limestone. The Yarrangobilly Limestone is very compact and has finely crystalline (dark limestone) to coarsely crystalline (pale limestone) fabric (texture) due to its diagenetic history. Permeability is related to fracture and fissure networks that allow flow through the karst unsaturated zone (see Fig. 1d in Markowska et al., 2015). Situated in the Snowy Mountains subalpine region, Harrie Wood Cave is distinct from other southeastern New South Wales karst sites; most notably, the study site

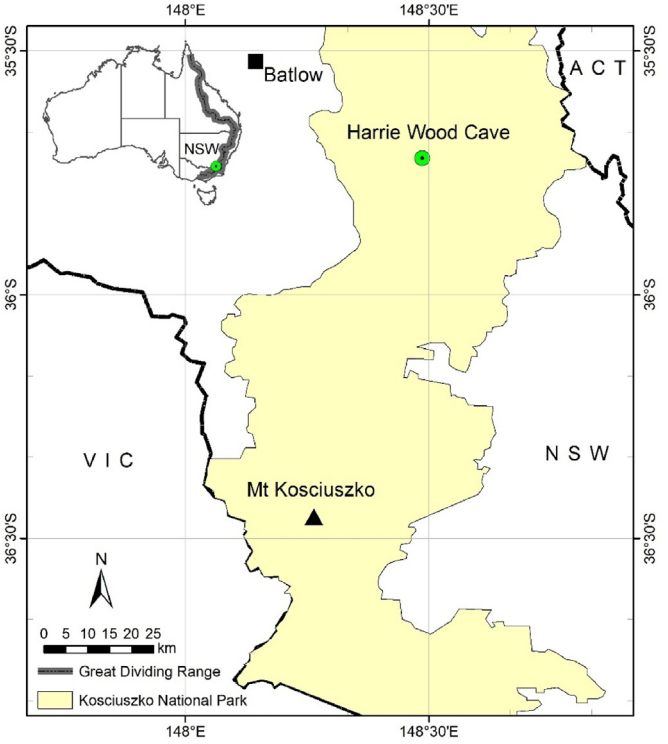

Fig. 1. Location map of the long-term climate station at Batlow Post Office (BoM station 072,004) and Harrie Wood Cave in the north of Kosciuszko National Park, which boarders with the Australian Capital Territory (ACT), south-eastern New South Wales (NSW), and eastern Victoria (VIC).

lies on the western side of the Great Dividing Range, with topographic relief of ca. 1100 m above sea level (a.s.l) and is in a temperate montane climate.

Harrie Wood Cave is a south-ward dipping cave, approximately 80 ± 2 m in length and 34 ± 1 m deep (Nicholl, 1974), and is hosted within fractured limestone. The cave entrance is ≈ 965 m a.s.l on a north/north-west facing steep rocky gorge, the general land surface slope dip is ≈ 30°. Vegetation cover above the cave is sparse and surrounding vegetation consists of open snowgum and black sallee woodland with a snow grass dominated understorey (Aplin et al., 2010). Wildfires are common in this region, with the area above the cave having completely burnt in 2003 CE and 2020 CE wildfires, although Coleborn et al. (2018, 2019) have shown that drip water geochemistry appears to be unaffected by fire (at least low intensity) in these deeper cave systems at Yarrangobilly. The soil above the cave is relatively shallow ≈0–0.5 m deep, lacking clearly defined horizons and is dominated by angular limestone clasts (typically sized 2–10 cm), indicating mechanical weathering processes. Harrie Wood Cave has an interior mean cave air temperature of 11.3 ± 0.1 °C (Markowska, 2012) and an average relative humidity of 91 ± 5% (2014–2017; Tadros et al., 2016).

The mean annual outside air temperature is 10.5 ± 0.5 °C and ranges from −1.8 ± 3.6 °C in July to 27.8 ± 4.2 °C in January (1985–2013; BoM, 2022). Median annual rainfall is 1178 ± 258 mm yr^{-1} (1 s.d.), however annual precipitation ranges from 552 to 1528 mm (1985–2013; BoM, 2022). This variability is related to the influence of El Niño–Southern Oscillation phases (Risbey et al., 2009). Although rainfall amount varies significantly from year to year, precipitation and evapotranspiration (ET) regimes are associated with a consistently strong seasonal cycle in this temperate montane region. Maximum precipitation and soil moisture field capacity occur in austral winter when ET rates are at a minimum (Fig. 1c in Tadros et al., 2016, Fig. 3 in Tadros et al., 2019). Precipitation in winter mainly falls as rain with fewer than approximately 15 snow days per year. In addition, the minimum 7-day antecedent precipitation required to generate recharge and a drip discharge response varies seasonally from 15 to 25 mm in winter to >50 mm in February and March (Baker et al., 2021). A large increase in soil moisture occurs in early winter when the soil reaches field capacity. Within the monitored period, recharge occurred in all years but predominately via winter precipitation, and leads to increased winter drip discharge within Harrie Wood Cave. The drip water $\delta^{18}O$ reflects the weighted mean of precipitation $\delta^{18}O$ of −6.9‰ (2007–2013, Tadros et al., 2016; Baker et al., 2019).

2.2. Stalagmite records

Three actively forming stalagmites were extracted from Harrie Wood Cave (Fig. 2). HW-S1 and HW-S2 (width and length: 80 and 140 mm and 70 and 160 mm, respectively) were removed in mid-2006 from the middle section of the cave system, at a depth of 38 m to the surface (Tadros et al., 2016). HW_38 b, 30 mm wide and 66 mm in length, was collected in December 2013 from the deepest chamber, 52 m below the surface (Markowska et al., 2019). As noted in Markowska et al. (2019), the top 21 mm of HW-S1, 20 mm of HW-S2 and 10 mm of HW_38 b represent modern carbonate growth above unconformities, which are identified by a gap in deposition, and a clear breakage surface is evident in HW-S1. Only the modern section of the record is used here to investigate the stalagmites' $\delta^{18}O$ responses to recharge.

The chronologies of HW-S1, HW-S2 and HW_38 b reported by Markowska et al. (2019) are used in this investigation and were established using ^{14}C bomb-pulse age modelling. The age ranges of each interval of modern growth for HW-S1, HW-S2 and HW_38 b are 1922–2006 CE (total error: ± 1.8–3.54 yr), 1926 to 2006 CE (total error: ± 1.45 yr) and 1951 and 2013 CE (total error: ± 3.48 yr), respectively. Stalagmites HW-S1 and HW_38 b had a constant growth rate of 0.25 and 0.17 mm yr^{-1}, respectively. HW-S2 had variable growth rates of 0.22 mm yr^{-1} prior to 1959 CE, 0.14 mm yr^{-1} between the years 1959 CE and 1969 CE and 0.30 mm yr^{-1} from 1969 CE to present. Thin section images under plane-polarised light of the modern sections of the three stalagmites show that they predominantly consist of compact columnar calcite with layers of columnar porous (Cp in Supplementary Figure A1) and rare columnar microcrystalline (Cm in Supplementary Figure A1) fabric types. The compact columnar fabric is typically observed in stalagmites fed by constant drip rate and drip water that is slightly supersaturated with respect to calcite (SIcc 0.1 to 0.4), where the inflow of colloidal particulate is minimal and the Mg/Ca ratio is < 0.3 (Frisia, 2015); the columnar porous and microcrystalline types likely reflect periods with increased inflow of particulates (Chiarini et al., 2017).

2.3. Cave monitoring

Harrie Wood Cave relative humidity (accuracy of ±3%) was measured bi-monthly using a Kestrel 3000 Weather Meter, at the location of the HW2 drip water sampling site. Cave air temperature was determined using miniature temperature loggers (DST micro-T, Star Oddi; accuracy: ± 0.06 °C) suspended in the air, free from contact to drip sites or cave walls, over a 10-month monitoring program near sites HW1 and HW2 (Markowska, 2012). A comprehensive cave drip-water monitoring program at site HW1 and HW2 commenced after the stalagmites from the same drip sites were removed in mid-2006 CE. Data over the period July 2006 to December 2013 are published in Tadros et al. (2016) (see Section 2.1). Additionally, the drip rate at site HW_38 b was measured between 2012 and 2016 CE using a Stalagmate™ acoustic drip rate logger (Collister and Mattey, 2008). Drip water for this site was spot sampled from 2012 to 2015 CE, when sufficient dripping occurred, capturing water that discharged in the previous 1–36 h. Dripwaters were collected in 7 mL exetainer glass vials, filled all the way up to the brim for isotopic analysis (n = 8).

2.4. Regional rainfall and modelled recharge calculation

To examine long-term regional rainfall and to calculate infiltrating recharge to the aquifer above Harrie Wood Cave for the 1911–2017 CE interval, daily rainfall data from the long-term climate station at Batlow Post Office (BoM station 072,004) was used, as it is in close proximity to Yarrangobilly Caves (~37 km NW; Fig. 1) and has been continuously operational since 1886 CE.

Baker et al. (2021) calculated monthly rainfall recharge thresholds for this montane karst environment in the adjacent South Glory Cave. The hydrological flow regime in Harrie Wood Cave was observed to fall between the flow regime of stalagmite drip sites (G3, G6, G8, G10, M1, M4, M13, M14) and the monitored flowstone (LR1) in South Glory Cave (see Supplementary Figure A3). As such, the monthly 7-day minimum precipitation amount for 'all sites except LR1' and 'all sites', as tabulated in Table 2 of Baker et al. (2021), were used to represent the lower and upper limit of recharge in Harrie Wood Cave, respectively.

Following Baker et al. (2021), first, a 7-day running sum of precipitation was calculated until this exceeded the monthly 7-day minimum precipitation. Next, recharge was estimated by subtracting the 7-day minimum precipitation from the 7-day running sum of precipitation, and the 7-day running sum calculation was reset to zero. Finally, monthly and yearly recharge time series beginning from 1911 CE was calculated by summing the daily recharge. The mean recharge (monthly or annual) between the

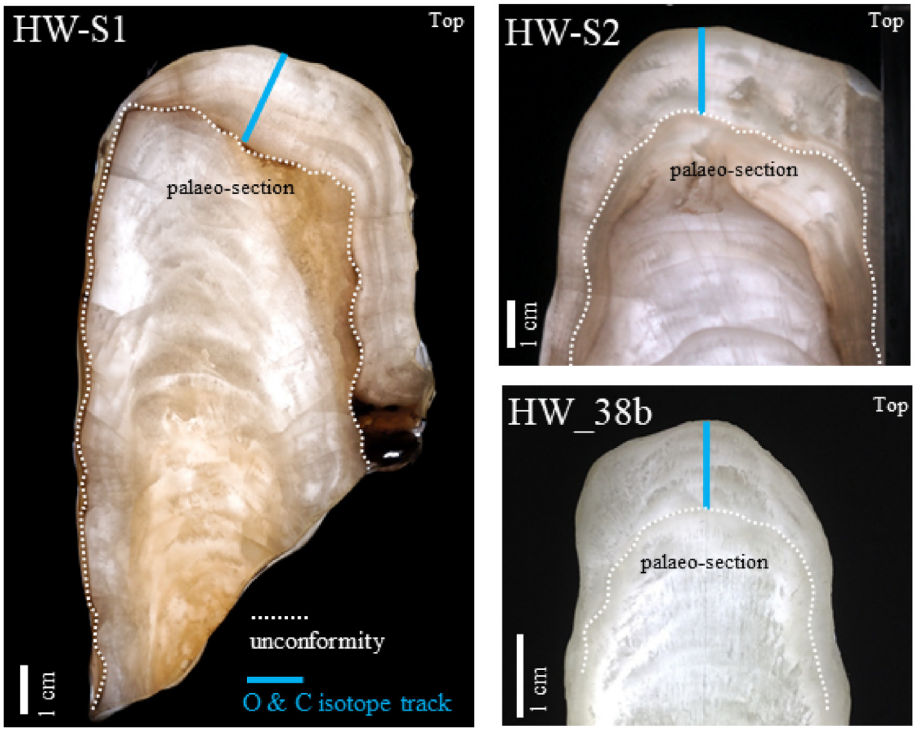

Fig. 2. Cut and polished thick sections of stalagmites HW-S1, HW-S2 and HW_38 b from Harrie Wood Cave. The white dotted lines mark the unconformity between the "palaeo-section" (older Holocene) and modern growth. Blue solid line in the modern growth indicates transect where powders were micromilled for isotope ($\delta^{18}O$ and $\delta^{13}C$) analyses (see Section 2.5). (For interpretation of the references to colour in this figure legend, the reader is referred to the Web version of this article.)

lower ('all sites except LR1') and upper ('all sites') limit of recharge was reported with its uncertainty, to provide the range of modern recharge for Harrie Wood Cave.

2.5. Stalagmite carbonate micro-sampling

Slices approximately 7 mm thick were cut from the central growth axes of stalagmites HW-S1, HW-S2 and HW_38 b, respectively, and then halved along the growth axis. Using a 2-mm diameter tungsten carbide mill end, carbonate powders were milled continuously along the growth axis of each stalagmite in 0.1 mm increments, cutting 2 × 2 mm along the growth laminae, using a TAIG micro-mill. Milling transects for high-resolution isotopic analysis are shown in Fig. 2 (HWS1: n = 282, HW-S2: n = 200, HW_38 b: n = 108). The temporal resolutions of HW-S1 and HW-S2 and HW_38 b is ~3 and ~2 data points per year, respectively.

2.6. In-cave calcite precipitation experiments

The isotopic compositions of modern (farmed) calcite end-members were taken as a direct test for isotope equilibration during calcite precipitation. Farmed calcite precipitated on artificial substrates over three-month intervals was harvested from the central part of the drip impact zone for isotopic analysis. Sand-blasted and laser cut plastic circular truncated cone substrates (bottom diameter = 34 mm with 4 notches in the perimeter of the base to allow drip water flow through; top diameter = 27 mm; height = 5 mm) were placed in the plastic funnel underneath drip sites HW1 (n = 7) and HW2 (n = 6). While 60 mm diameter glass plates, convex side up, were placed under stalactite HW_38 b (n = 4).

Two instant precipitation experiments were also carried out in the cave following the protocol described in Frisia et al. (2018) to illustrate the first phase of crystallization from drips HW1 and HW2. The results of the experiments were observed on a JEOL 2100 LaB_6 instrument equipped with STEM and EDS systems at the Electron Microscope and X-Ray Unit of the University of Newcastle (Supplementary Figure A2).

2.7. Stable isotope analysis ($\delta^{18}O$ and $\delta^{13}C$)

The oxygen and carbon isotope composition of calcium carbonate powders from HW-S1 (mass range: 0.7–0.8 mg) were analysed on a GV Instruments GV2003 continuous-flow isotope-ratio mass spectrometer (IRMS) at the Discipline of Earth Sciences, University of Newcastle, Australia. The samples were digested in 105% phosphoric acid at 70 °C and mass spectrometric measurements made on the evolved CO_2 gas. Results were normalised to the Vienna-Pee Dee Belemnite (VPDB) scale using an internal working standard (Carrara Marble standard NEW1 – prepared at U. Newcastle) previously calibrated using the IAEA National Bureau Standards: NBS-18 ($\delta^{18}O = -23.20‰$ and $\delta^{13}C = -5.01‰$) and NBS-19 ($\delta^{18}O = -2.20‰$ and $\delta^{13}C = +1.95‰$). Mean uncertainty (1 s.d.) on NEW1 was 0.03‰ and 0.09‰ for $\delta^{13}C$ and $\delta^{18}O$, respectively.

Stable isotope analyses of carbonates ($\delta^{13}C$ and $\delta^{18}O$) from HW-S2, HW_38 b and farmed calcite were performed on the MAT-253 IRMS equipped with a Kiel IV carbonate device (Thermo Scientific, Bremen, Germany) at the Mark Wainwright Analytical Centre at UNSW Sydney. Approximately 20–40 μg sub-samples were digested in 2 drops of 100% phosphoric acid at 70 °C. The Kiel IV carbonate device settings used were a reaction one time of 420 s, a reaction two time of 120 s and a transfer time of 90 s. An integration time of 16 s and 8 cycles was used for the isotopic measurement of CO_2 gas. Data were normalised to the VPDB scale using a two-point calibration against NBS-18 and NBS-19. The analytical precision of the standards calculated for these datasets was 0.05‰ and 0.06‰,

for $\delta^{13}C$ and $\delta^{18}O$, respectively. The chronologies for the three stalagmites are published in Markowska et al. (2019) and employed in this paper (see Section 2.2).

Stable isotope analysis of drip water and rainfall samples ($\delta^{18}O$) was performed on a Picarro Cavity Ring-Down Spectrometer at ANSTO, Lucas Heights, Australia (reported accuracy of ±0.15‰ for $\delta^{18}O$). Each analysis run consisted of 62 drip water samples, 7 duplicates, 15 standards and 11 quality control samples. Every sample was analysed 7 times and corrected for memory. $\delta^{18}O$ values were normalised to in-house calibration standards AILS-006 ($\delta^{18}O$ = 7.60‰ ± 0.08) and AILS-008 ($\delta^{18}O$ = −22.12‰ ± 0.07), which are standardised to VSMOW2 and SLAP.

2.8. Calculation of oxygen fractionation factors for Harrie Wood Cave calcites

The isotopic fractionation that occurs between drip water and calcite during precipitation is expressed as a fractionation factor, α. The α values for the three speleothem sites were calculated using the measured $\delta^{18}O$ values of farmed calcite and its feeding drip water by using the following relation:

$$^{18}\alpha_{(\text{calcite}-\text{water})} = \frac{\delta^{18}O_{calcite} + 1000}{\delta^{18}O_{water} + 1000} \quad [1]$$

Where both the $\delta^{18}O$ value of calcite and water are relative to the VSMOW scale (Coplen, 2007).

The deviation of α from 1, or fractionation $^{18}\varepsilon$ (‰) is:

$$^{18}\varepsilon = \left(^{18}\alpha_{\text{calcite}-\text{water}} - 1\right) \times 1000 \quad [2]$$

The $\delta^{18}O$ (VPDB) values were converted to the VSMOW scale using the equation given by Coplen (1988):

$$\delta^{18}O\ (\text{VPDB}) = (0.97001\ \text{x}\ \delta^{18}O\ (\text{VSMOW})) - 29.99‰ \quad [3]$$

The cave drip water $\delta^{18}O$ (VSMOW) values measured from samples collected in the period when calcite was farmed were compared to a calcite-equivalent $\delta^{18}O_{dw}$ value (VPDB). The calcite $\delta^{18}O$ value expected in isotopic equilibrium conditions with the parent fluid (diagonal striped box in Fig. 3c) was calculated using the Kim and O'Neil (1997) α value at the mean observed cave air T in degrees Kelvin (°K):

$$\text{calcite-equivalent}\ \delta^{18}O_{dw}\ (\text{VSMOW}) = [e^{[(18.03/T) - (32.42/1000)]}\ \text{x}\ (\delta^{18}O_{dw}\ (\text{VSMOW}) + 1000)]\text{-}1000 \quad [4]$$

The calcite-equivalent $\delta^{18}O_{dw}$ (VSMOW) is then converted to VPDB using equation (3).

The measured Harrie Wood Cave α values were then compared to fractionation factors in the literature (e.g., Kim and O'Neil, 1997; Tremaine et al., 2011; Johnston et al., 2013; see Section 3.1).

3. Results

3.1. Drip water, stalagmite and farmed calcite variability

Box plots of drip rate, $\delta^{18}O_{dw}$, and stalagmite $\delta^{18}O$ and $\delta^{13}C$ from the three sites are shown in Fig. 3 (see Supplementary Table A1 for summary statistics). Median drip rates show considerable variation between the three sites (Fig. 3a). Drip site HW1 has the highest median drip rate of 0.86 ± 0.23 drips min^{-1} (1σ). HW2 drip rate is similar but with higher variability: 0.68 ± 0.70 drips min^{-1}. HW_38 b has the lowest median drip rate and variability: 0.13 ± 0.05 drips min^{-1}.

The median $\delta^{18}O_{dw}$ values of HW1 and HW2 are similar (HW1 $\delta^{18}O_{dw}$ = −6.9 ± 0.2‰; HW2 $\delta^{18}O_{dw}$ = −6.8 ± 0.3‰; Fig. 3c), although the interquartile range is larger and maximum value is higher for HW2 (0.3‰ and −6.0‰, respectively) compared to HW1 (0.2‰ and −6.5‰, respectively). HW_38 b, the slowest dripping site, displays the highest median $\delta^{18}O_{dw}$ value (−6.6 ± 0.1‰), but is within 1σ error of the other two sites.

Comparing speleothem isotopic values shows that $\delta^{18}O_{stal}$ values for all three speleothems are similar (HW1: −5.7 ± 0.4‰; HW2: −5.5 ± 0.4‰; HW_38 b: −5.4 ± 0.3‰; II in Fig. 3c), while HW_38 b has a higher median $\delta^{13}C$ value (−6.1 ± 1.3‰) versus HW1 and HW2 (−7.5 ± 1.1‰ and −7.2 ± 0.8‰, respectively) (Fig. 3b). The farmed calcite $\delta^{18}O$ values (red square windows in Fig. 3c) overlap and exceed the higher end of the observed stalagmite $\delta^{18}O_{stal}$ values (II in Fig. 3c) and is consistent with a trend towards higher values at the time when the stalagmites were harvested and calcite farming began (Fig. 4).

The farmed calcite oxygen isotope fractionation factor value, $^{18}\alpha_{(\text{calcite-water})}$, determined from HW1 (1.033; $^{18}\varepsilon$ = 32.8‰), HW2 (1.033; $^{18}\varepsilon$ = 32.7‰) and HW_38 b (1.032; $^{18}\varepsilon$ = 32.4‰) varies from the Kim and O'Neil (1997) $^{18}\alpha_{(\text{calcite-water})}$ of 1.031 at 11.3 °C ($^{18}\varepsilon$ = 31.4‰; see Section 2.8). The mean farmed calcite $\delta^{18}O$ values are 1.4‰ higher for sites HW1, HW2 and HW_38 b versus the calcite-equivalent $\delta^{18}O_{dw}$ values predicted by the Kim and O'Neil (1997) fractionation factor (diagonal striped boxes in Fig. 3c). The higher oxygen isotope fractionation factors between farmed calcite and water observed in Harrie Wood Cave is however in good agreement with published $^{18}\alpha_{(\text{calcite-water})}$ values from calcite precipitated in other natural cave systems at comparable cave temperatures (e.g., Tremaine et al., 2011; Johnston et al., 2013) compared to fractionation factors determined in laboratory experiments (e.g., Kim and O'Neil, 1997). Furthermore, the empirical oxygen isotope fractionation factors for HW1, HW2 and HW_38 b are consistent across the three sites, despite the difference in drip rate, which may be a consequence of similar growth processes.

3.2. Stalagmite $\delta^{18}O$ time series

The $\delta^{18}O$ time series record for stalagmites HW-S1, HW-S2 and HW_38 b over the years: 1922 to 2006 CE, 1926 to 2006 CE and 1951 and 2013 CE, respectively, are compared in Fig. 4. There is broad agreement between the records on multi-decadal timescales with high isotopic values prior to 1950 CE, followed by lower values until 1990 CE, and rising values thereafter.

During the 1960s, 1970s and 1980s, mean HW-S1 values are −5.9 ± 0.3‰, −6.1 ± 0.2‰; and −6.1 ± 0.2‰, respectively. The corresponding HW-S2 values are higher but within 1 s.d. (1σ) of HW-S1 (1960s: −5.4 ± 0.3‰; 1970s: −5.8 ± 0.2‰; 1980s: −6.1 ± 0.2‰). Mean HW_38 b $\delta^{18}O$ values during the 1960s are also within 1σ (−5.6 ± 0.2‰), however there is less agreement between mean HW_38 b $\delta^{18}O$ values during the 1970s (−5.3 ± 0.1‰) and 1980s (−5.5 ± 0.2‰), when HW_38 b values are higher than HWS1 and HW-S2 by 0.4‰–0.7‰. All three records demonstrate a rising trend since approximately 1990 CE. The timing of the post-1990 rise in $\delta^{18}O_{stal}$ is approximately five years later for HW-S1, although this could be due to uncertainty in the age models. The farmed calcite $\delta^{18}O$ values and HW1 drip water $\delta^{18}O$ values (as calcite equivalent) are also shown on Fig. 4 and are similar to the range of values for the three stalagmites since the late 1990s. Overall, the last two decades have the highest speleothem, drip water and farmed calcite $\delta^{18}O$ values for the 20th and 21st

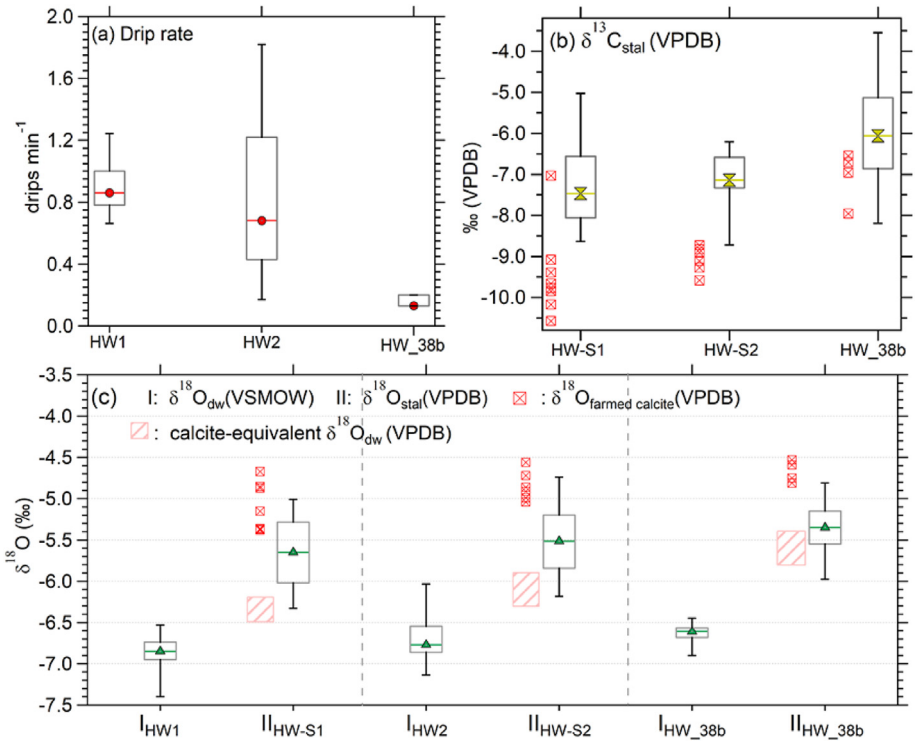

Fig. 3. Box plots of: (a) drip rate; (b) stalagmite $\delta^{13}C_{stal}$ values; and (c) drip water $\delta^{18}O_{dw}$ (I) and stalagmite $\delta^{18}O_{stal}$ (II) values for the three studied sites in Harrie Wood Cave. The lower, upper, and middle lines of boxes correspond to the 25th percentile, 75th percentile, and median, respectively. The whiskers at the top and bottom extend from the 95th and 5th percentiles, respectively. Red square windows in (b) and (c) correspond to farmed calcite $\delta^{18}O$ and $\delta^{13}C$ values, respectively. The diagonal striped box in (c) represents the range of $\delta^{18}O_{dw}$ values calculated on the calcite-equivalent (VPDB) scale (Equation (3)). (For interpretation of the references to colour in this figure legend, the reader is referred to the Web version of this article.)

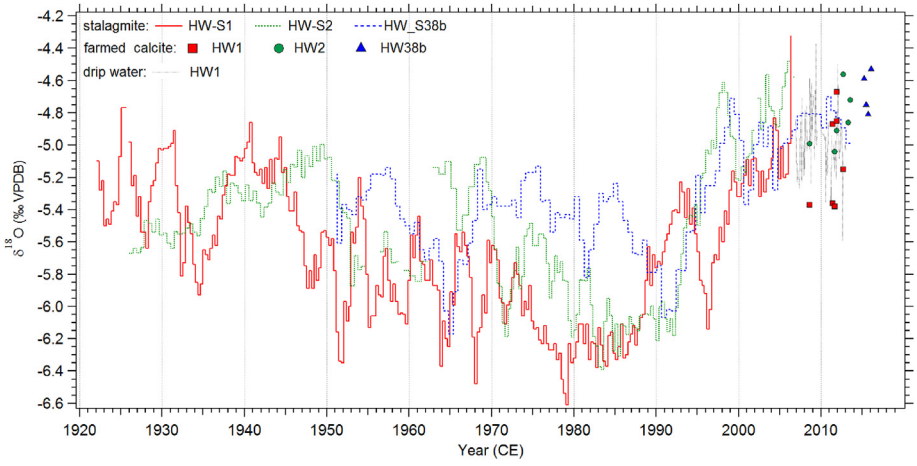

Fig. 4. Oxygen isotopic records of stalagmites HW-S1, HW-S2 and HW_38 b from Harrie Wood Cave. Solid squares, circles and triangles represent farmed calcite samples. The grey dashed line is the time series record of HW1 $\delta^{18}O_{dw}$ values converted to VPDB by applying the HW1 fractionation factor, $^{18}\alpha_{(calcite\text{-}water)}$ of 1.033 (Equation (1); section 3.1).

century period. These values exceed the $\delta^{18}O$ maxima recorded earlier in the record, i.e., mid-1920s, early 1930s and the late-1930s through 1940s.

When comparing the $\delta^{18}O$ time series of overlapping periods, the inter-annual variability of up to 1.4‰ observed in HW-S1 is not always captured in stalagmites HW-S2 and HW_38 b. For example, through the mid-1940s, the 1960s and mid-1990s, when the HW-S1 record isotopically decreases, the HW-S2 and HW_38 b records remain at higher values (Fig. 4). This is also the case with the farmed calcites for the period of cave monitoring, with HW1 being approximately 0.4‰ lower than HW2 and 0.6‰ lower than HW_38 b during the period 2008–2012 (solid squares, circles and triangles in Fig. 4). It appears that HW-S1 is more likely to record isotopic minima, and the extended cave monitoring dataset will be investigated further to understand this in Section 3.3.

Time series of the HW-S1 $\delta^{13}C$ record and associated $\delta^{18}O$ profile is shown in Supplementary Figure A4(b). The inter-annual trends in $\delta^{13}C$ are similar to the $\delta^{18}O$ record, although the magnitude of change between minima and maxima is larger by ~2‰ for $\delta^{13}C$ than in $\delta^{18}O$. There are short-lived periods (<3 years) within the time series that show a strong correlation between $\delta^{18}O$ and $\delta^{13}C$ (Supplementary Figure A4(a)), however overall, there is a weak but

significant relationship between $\delta^{18}O$ and $\delta^{13}C$ for each of the three stalagmites (HW–S1: r = 0.53; HW-S2: r = 0.35; HW_38 b: r = 0.19; p-value = 0; Supplementary Figure A5).

3.3. Drip water response to recharge

In this section, the modelled recharge time series (see Section 2.4) is presented and compared with observations for the monthly $\delta^{18}O$ precipitation-weighted mean (PWM $\delta^{18}O$), drip water Cl^-, $\delta^{18}O$ and drip rate datasets for site HW1 and HW2 and normalised drip rate for all monitored drip sites in Harrie Wood Cave (Fig. 5). It should be noted that the PWM $\delta^{18}O$ and drip water Cl^-, $\delta^{18}O$ and drip rate time series from November 2006 to December 2013 for these sites were presented in Tadros et al. (2016) and are extended here to April 2017. Tadros et al. (2016) reported that there is no consistent seasonality in the associated drip water Cl^- or $\delta^{18}O$ (Fig. 5). Rather, the key features of the drip hydrochemical time series are the increased variability and range of $\delta^{18}O_{dw}$ values during an uninterrupted dry period (Millennium Drought) and shifts to lower Cl^- and $\delta^{18}O_{dw}$ values during periods of pronounced recharge.

Comparisons of modelled monthly recharge data over the period of cave monitoring show that the modelled recharge reasonably represents the magnitude and timing of variations in discharge. Recharge of karst stores typically occurs in winter and is indicated when drip rates display an increase, i.e., a hydrograph-type response (Section 2.1; light blue bars in Fig. 5e and f). Winter recharge occurs every year to HW1, and to a lesser extent HW2, even throughout the Millennium Drought. In addition to the main recharge event reported in Tadros et al. (2016) during the 2010–12 La Niña, and indicated on Fig. 5 as recharge scenario (i), a further main recharge event is observed in the extended data from May 2016 to November 2016 (recharge scenario (ii) in Fig. 5) during a wet period of above-average rainfall conditions and the wettest interval since 2010–12 (BoM, 2022). Overall, HW1 typically records a relatively higher drip-rate response to recharge compared with HW2, which suggests that the flow path to HW1 may have a more direct connection with the surface and that the drip water is supplied from a larger store volume relative to HW2. This is supported by the more frequent occurrence of porous fabric layers in HW-S1 than in HW-S2 and HW_38 b and the results from the instant precipitation experiments (see Supplementary Figure A2) conducted during recharge scenario (ii). The more frequent porous Cp fabric is related to higher particulate inflow (see Supplementary Figure A1), which is likely associated with drip rates faster than the those associated with compact columnar (Cc). The presence of colloidal particles captured on the TEM grids, with HW1 being richer in soil-derived particulates, indicates transport along preferential fissures and solutionally enlarged fracture-flow networks (see Supplementary Figure A2).

The hydrochemistry dataset of Tadros et al. (2016), here extended from 2014 to 2017, captures additional hydroclimate variability that when combined with the new modelled recharge timeseries calibrated using site data, assists in the interpretation of the stalagmite records presented here. For the 10-year monitored period (November 2006–April 2017), the mean modelled monthly recharge is 27 mm $month^{-1}$ (range: 0–187 mm $month^{-1}$). The impact of the Millennium Drought (from late 1996 to mid-2010 CE) on the monitoring data was previously described in Tadros et al. (2016) and mean modelled monthly recharge calculated for this investigation was 19 mm $month^{-1}$ (November 2006 CE – May 2010 CE). In the extended dataset, a second multi-year dry interval occurred from July 2014 CE until April 2016 CE, when mean modelled monthly recharge was 15 mm $month^{-1}$ (Fig. 5). Considering the extended dataset, drip rates were still at their lowest for the observed period (HW1 minimum = 0.33 drips min^{-1}; HW2 minimum = 0.08 drips min^{-1}) during the Millennium Drought.

Tadros et al. (2016) demonstrated that the drip water isotopes

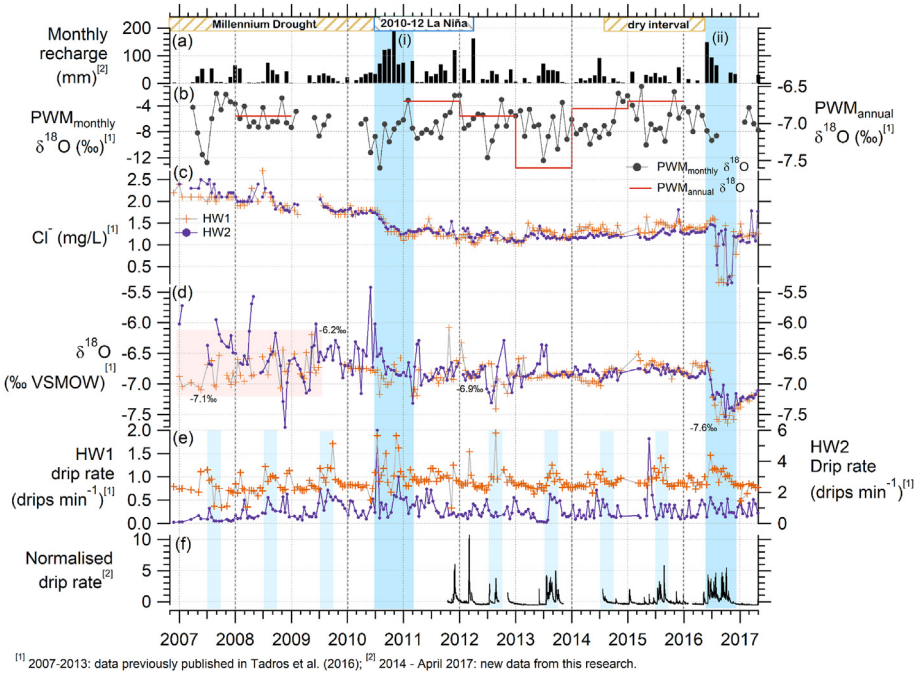

Fig. 5. Time series of: (a) modelled monthly recharge; and (b) monthly $\delta^{18}O$ precipitation-weighted mean (PWM $\delta^{18}O$; black circles) values, with the red line indicating the amount-weighted annual $\delta^{18}O$-values for complete years of precipitation data. Time series of: (c) drip water Cl^- concentrations; (d) drip water $\delta^{18}O$ values; and (e) drip rate for drip sites HW1 (orange crosses) and HW2 (purple circles), and (f) Normalised drip rate for 12 monitored drip sites within Harrie Wood Cave, including HW_38 b, measured using Stalagmate™ drip loggers. Blue panels represent recharge periods of karst water stores in Harrie Wood Cave. The red panel represents the period of low recharge. (For interpretation of the references to colour in this figure legend, the reader is referred to the Web version of this article.)

fall along the local meteoric water line for this site (their Fig. 4). This also holds in the extended dataset (Supplementary Figure A6) indicating that the karst stores reflect recharge from rain events. Drip Cl^- and $\delta^{18}O$ values are higher during the Millennium Drought (Cl^-: HW1 = 1.96 ± 0.19 mg/L; HW2: = 2.00 ± 0.23 mg/L; $\delta^{18}O$: HW1 = −6.8 ± 0.2‰; HW2 = −6.5 ± 0.4‰) than at any time during the extended dataset (Cl^-: HWl = 1.26 ± 0.26 mg/L; HW2 = 1.24 ± 0.21 mg/L; $\delta^{18}O$: HW1 and HW2 = −6.9 ± 0.2‰). The PWM $\delta^{18}O$ value is also higher in the Millennium Drought (−6.8‰) and in the second dry interval (−5.9‰), than the average annual PWM $\delta^{18}O$ (−7.0‰). Tadros et al. (2016) described the drip water as having relatively higher variability in $\delta^{18}O_{dw}$ values during the Millennium Drought and this is still the case in the context of the now longer dataset. This suggests that $\delta^{18}O_{dw}$ during drier periods may have been responsive to intermittent recharge events with mixing potential reduced by a depleted karst store.

The conclusion of the Millennium Drought and the second dry interval are marked by a decrease in Cl^- and $\delta^{18}O_{dw}$ values indicating recharging of the karst stores (Tadros et al., 2016). A second major recharge event (May 2016 to November 2016) produced a larger decrease in $\delta^{18}O$ (1‰ VSMOW) and in Cl^- (92%) compared with the conclusion of the Millennium Drought when the response was 0.4‰ and 62%, respectively. The overall magnitude of the response for the two drip sites is the same but is delayed in HW2 by five months, consistent with our hypothesis that HW1 has a more direct connection with the surface. Prior to this recharge, Cl^- concentrations from 2011 to 2016 are less variable (HW1 = 1.24 ± 0.26 mg/L; HW2 = 1.22 ± 0.20 mg/L). There is a rise in drip water HW1 $\delta^{18}O$ values (~0.5‰), although PWM $\delta^{18}O$ values are also higher by ~0.8‰ through this period. After recharge, drip $\delta^{18}O$ values fall to −7.6‰, well below the average annual PWM of −7.0‰. Comparing the relative response of drip $\delta^{18}O$ to the two major recharge scenarios suggests that the karst stores were more depleted prior to the second major recharge event versus the first. The reason for this is not entirely clear but could be due to the cumulative impact of successive droughts on overall recharge to the karst stores and the post-Millennium Drought recharge being insufficient to fully recharge stores.

Overall, these field observations from long term monitoring confirm that HW1 and HW2 are responding to recharge events, with HW1 relatively more responsive to recharge, in terms of magnitude and timing, compared to HW2. These considerations also agree with the three stalagmites' $\delta^{18}O$ records, i.e., more frequent and larger-magnitude negative $\delta^{18}O$ excursions are clearly recorded in stalagmite HW-S1 compared to HW-S2 and HW_38 b (Fig. 4).

3.4. Comparison of the HW-S1 $\delta^{18}O$ record to the regional rainfall and modelled recharge record

Fig. 6 shows time series of Victorian and regional rainfall anomalies during the cool season (Apr–Oct), modelled recharge and HW-S1 $\delta^{18}O$ values for the period from 1922 CE to 2006 CE. The higher resolution $\delta^{18}O$ data from the HW-S1 record (Section 3.2) and the enhanced response of site HW1 to recharge events during the monitoring period (Section 3.3) suggest that HW-S1 responds within a short time to recharge and is, as such, better suited for recording an infiltration signal in the last ca. 100 years. For this reason, Fig. 6c and d compares the modelled annual recharge with the HW-S1 $\delta^{18}O$ stalagmite record between 1922 CE and 2006 CE,

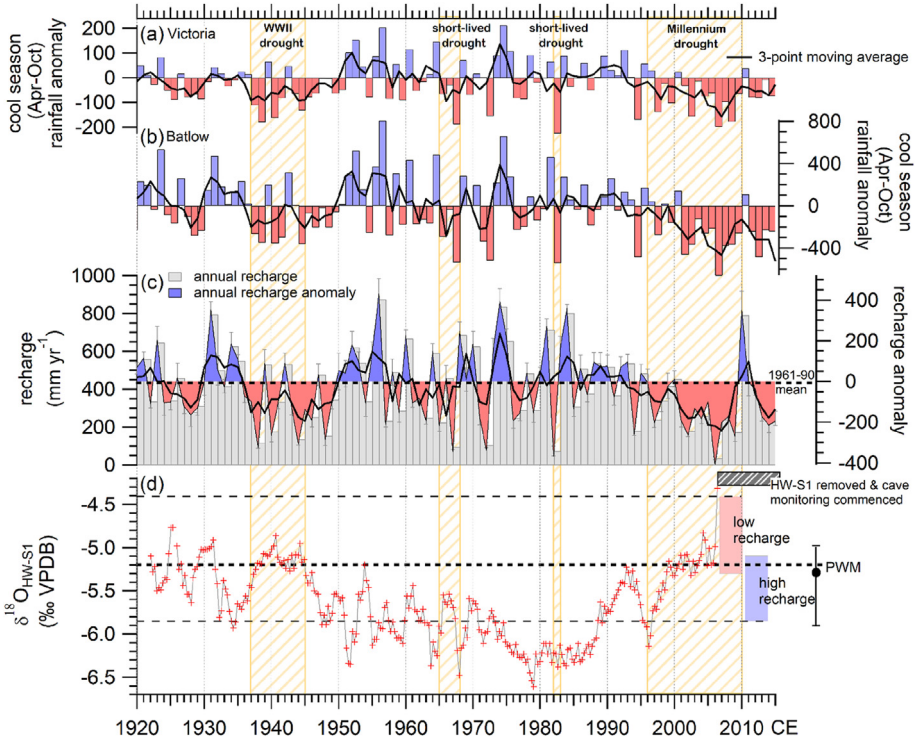

Fig. 6. (a) Victorian annual (Apr–Oct) cool-season rainfall anomaly (BoM, 2022). (b) Regional cool season (Apr–Oct) rainfall anomaly relative to the 1961–1990 mean of 903 ± 299 mm yr^{-1} over Batlow (BoM station 72,004) for the 1920–2015 CE period. (c) Annual mean modelled recharge (± recharge range; Section 2.4) and annual recharge anomaly from the 30-year (1961–1990) average of 442 ± 204 mm yr^{-1} (dotted line; negative anomalies in red, positive anomalies in blue). (d) Stalagmite HW-S1 $\delta^{18}O$ record for the period 1922–2006 CE. The pink bar represents the range of $\delta^{18}O_{dw}$ values during the monitored dry period, while the blue bar represents the range of $\delta^{18}O_{dw}$ values after recharge. Dashed horizontal line is the $\delta^{18}O$ PWM with error bars indicating the range of annual values. The $\delta^{18}O$ PWM and drip water (‰ VPDB) values in (b) were calculated using the $^{18}\alpha_{(calcite\text{-}water)}$ determined for HW1 (1.032; Section 3.1). (For interpretation of the references to colour in this figure legend, the reader is referred to the Web version of this article.)

respectively. The range in observed drip water $\delta^{18}O$ values for this site is also shown for the period of low recharge (November 2006 to mid-2010) versus the period of higher recharge (recharge scenario (i) and (ii) in Fig. 5).

The modelled recharge timeseries closely follows the regional cool season rainfall anomalies (Fig. 6c and b, respectively). This is consistent with the monitoring data that demonstrates an enhanced drip rate response to cool season recharge and the broader regional alpine record (Fig. 6a; Rauniyar and Power, 2020). In general, the region experienced below-average rainfall in the mid-1920s and during the World War II Drought (1936–45 CE). Over the 1950 to mid-1990 period the region experienced mostly above-average rainfall that was interrupted by rainfall deficiencies of up to three years, and short-lived drought periods (1965–1968 CE–1983 CE). From 1993 CE and by the Millennium Drought (late 1996 to mid-2010 CE) the effect of successive below-average rainfall was cumulative, and the region experienced a sustained decline in cool-season rainfall until the very strong 2010–2011 La Niña event. These changes in cool-season rainfall anomalies directly impact recharge to karst aquifers.

Annual modelled recharge estimates for the period from 1920 to 2015 CE (Fig. 6c) is positive for all years, indicating there were no years during this period when recharge did not occur to Harrie Wood Cave. There is considerable interannual variability in recharge; however, when compared to the 30-year mean annual recharge (1961–1990; 442 ± 204 mm yr^{-1}), there are periods when recharge conditions are consistently higher or lower-than-average. Long periods of high recharge (positive recharge anomalies) generally occur in the early 1930s, 1950–1956 CE, late 1960s, mid 1970s and early 1980s to early 1990s. Successive years of low recharge are recorded in 1924–1930 CE, from 1936 to 1949 CE during the WWII drought, and in 1961–1967 CE. The modelled data indicate Harrie Wood Cave experienced the longest period of low recharge during the Millennium Drought, from 1994 to 2009 CE, with recharge falling to its lowest in 2006 CE. Although this is the most extensive dry period since 1920 CE, the modelled data suggests recharge was enough to sustain baseflows to support constant growth through this period; field observations confirm the stalagmites were fed from actively drips when removed in 2006 CE (Section 2.2).

During the first two decades of observed speleothem growth, annual modelled recharge is mostly at or higher than the 30-year average (442 ± 204 mm yr^{-1}; dotted line in Fig. 6c) except for 1926–1930 CE. Speleothem $\delta^{18}O$ values are typically lower than the PWM value and coincide with higher modelled recharge in the 1930s, apart from a short-lived maximum around 1925 CE and during 1929–1932 CE, the latter coinciding with the five years of reduced modelled recharge. Site recharge is lower through the WWII Drought and the response of HW-S1 to this drought is higher $\delta^{18}O$ values than the PWM and consistent with the range of drip-water $\delta^{18}O$ values (as calcite-equivalent) when low recharge was experienced during the first half of the monitored period (pink bar in Fig. 6d).

Towards the end of the WWII Drought, annual recharge falls to 136 mm in 1944 CE, then increases three-fold from 1945 to 1947 CE. This recharge period corresponds with an ~0.7‰ drop in stalagmite $\delta^{18}O$ values. From 1948 CE until the late-1980s annual recharge generally varies between 2 and 3 years of consecutive above-average recharge and 1–2 years of below-average recharge. Likewise, HW-S1 $\delta^{18}O$ values also fluctuate inter-annually under these changing recharge conditions by approximately 0.5–1‰. During this period HW-S1 $\delta^{18}O$ values remain below the long-term PWM and are lower than or consistent with the range of drip water $\delta^{18}O$ values (as calcite-equivalent) experienced during the period of high recharge that occurred in the monitoring interval (blue bar in Fig. 6d). The periods of high recharge anomalies listed above can generally be matched with low stalagmite $\delta^{18}O$ values i.e., 1950-56 CE, late 1960s, mid-1970s, although it is difficult to make a confident close comparison owing to the uncertainty in the HW-S1 age model. Two-short-lived droughts were experienced in this mid-century period (Fig. 6). Although $\delta^{18}O$ values increased in response to the event in the 1960s, these values are still lower than the PWM and lower when compared with HW-S1 values during longer droughts. This demonstrates the insensitivity of the speleothem to record short-lived droughts when the karst has enough water stored from previous years and is replenished in the subsequent wetter years.

HW-S1 $\delta^{18}O$ values return to the PWM from the late 1980s until 1993 CE during a period of average recharge (Fig. 6) consistent with the antiphase behaviour between speleothem $\delta^{18}O$ and recharge elsewhere in the record and our observations in the monitored period. From 1994 to 1995 CE the site recharge increased by 302 mm and HW-S1 $\delta^{18}O$ values decreased below the long-term PWM to values previously recorded during periods of high-recharge anomalies. From the mid-1990s and through the prolonged Millennium Drought, HW-S1 $\delta^{18}O$ values rise by ~1.3‰. These results are at or higher than the PWM and are consistent with the subsequent drip-water $\delta^{18}O$ values observed during the Millennium Drought (pink bar in Fig. 6d).

It is likely that a reduction in rainfall associated with changes in dominant regional-scale climate patterns - namely strong El Niño-drought conditions (1925-26 CE and 1940-42 CE), moderate to strong El Niño events (1963, 1965, 1972, 1977 and 1982-83 CE) and drought periods (Theobald and McGowan, 2016) - contribute to a decline in site recharge. Evidently, the HW-S1 $\delta^{18}O$ record does not capture one-to two-year drought events, unless it occurs after a longer-duration dry interval when the total karst store volume has not had time to replenish. For example, correlations between recharge and the SOI and SAM climate indices are weak (τ varies between 0 and 0.3; see Supplementary Table A2) but statistically significant in winter and spring, indicating short-term ENSO or SAM events will not be captured by HW-S1 $\delta^{18}O$ as multi-year dry periods are needed to affect karst storage.

Hence, a comparison of the HW-S1 $\delta^{18}O$ time series to modelled recharge data as well as empirical data from cave monitoring provides evidence that increasing speleothem $\delta^{18}O$ values higher than the PWM occurs with decreasing recharge, while decreasing $\delta^{18}O$ values lower than the long-term PWM occurs in association with high recharge periods.

4. Discussion

4.1. Interpretation of $\delta^{18}O$ variability in modern Harrie Wood speleothems

The results of this research have shown that the $\delta^{18}O$ changes in HW-S1 respond to recharge of karst stores during periods of wetter hydroclimate. During periods of significant recharge, karst stores are replenished and drip/speleothem $\delta^{18}O$ values decrease below the amount-weighted rainfall $\delta^{18}O$ value determined over the monitoring period. We interpret that during low-recharge periods, infiltration to the karst stores is reduced but drips continue to be supplied by stored water. Below, we investigate two further potential processes behind the relationship between recharge and speleothem $\delta^{18}O$ response: enhanced disequilibrium and the impact of karst flow paths.

Oxygen isotopic disequilibrium between drip water and calcite $\delta^{18}O$ (Fairchild and Baker, 2012) is examined as a possible process for the observed relationship between recharge and speleothem $\delta^{18}O$, as longer drip intervals and/or prior calcite precipitation (PCP)

can enhance disequilibrium (Deininger et al., 2021). Tadros et al. (2016) identified the influence of PCP on Mg/Ca and Sr/Ca in drip waters in Harrie Wood Cave, although if PCP were impacting calcite $\delta^{18}O$ also, this would be evident as different $^{18}\alpha_{(calcite\text{-}water)}$ values between the sites. According to the hypothesis of Deininger et al. (2021), the consistency in oxygen isotope fractionation factors across the three speleothem sites (Section 3.1) suggests that there has been sufficient time for oxygen isotope exchange between HCO_3^- and H_2O to re-establish and is consistent with the interpretation presented in Tadros et al. (2016) that the process of PCP is occurring higher up in the karst flow path/store rather than on the stalactite. Furthermore, the instant precipitation experiments show that the drip water is sufficiently supersaturated that yields precipitation of calcite without much degassing (see Supplementary Figure A2).

We further examine if enhanced disequilibrium could be driving the relationship between recharge and speleothem $\delta^{18}O$ using the ISOLUTION model (Deininger and Scholz, 2019; see Supplementary Figure A7 for method). In the monitoring data, drip intervals fall to approximately 0.6–0.7 drips per min (100 s) during the Millennium Drought and other dry years e.g., 2015, for site HW1 (Fig. 5). Based on ISOLUTION modelled results, a departure to 100 s during a dry period would result in a modelled shift of approximately +0.2‰ (see Supplementary Figure A7(a)) whereas the rise in speleothem $\delta^{18}O$ in response to the Millennium Drought was much larger (approximately 1.3‰). At the maximum observed drip interval recorded for HW1 (182 s) the maximum modelled enrichment is still low (+0.3‰) and our monitoring data (Fig. 5) show that such extended drip intervals only occur <4% of the monitored period, which include during three years of the Millennium Drought. When the ISOLUTION modelled results are considered in a long-term context, the rainfall deficit during the Millennium Drought was the longest recorded within the period from 1920 CE to present (Fig. 6) and it is thus unlikely that these long drip intervals occurred during the growth period of speleothem HW-S1. Another stalagmite examined here, HW_38 b, did experience long drip intervals (median: 462 s; maximum: 857 s). The ISOLUTION results suggest that these longer drip intervals could result in precipitation of calcite with significantly enhanced isotopic values (a relative rise of +0.6‰ and +0.8‰ at the median and maximum drip intervals, respectively; see Supplementary Figure A7(b)). However, key features in the three coeval speleothem time series largely replicate (Fig. 4), and where discrepancies between the stalagmite records exist, it is during times of low $\delta^{18}O$ values (i.e., enhanced recharge). Furthermore, $^{18}\alpha_{(calcite\text{-}water)}$ data from the farmed calcites shows that the fractionation factors for each drip site are equivalent, so there is no evidence in our data to support that variability in speleothem $\delta^{18}O$ are driven by enhanced isotopic disequilibrium during low recharge periods.

Based on a seven-year monitoring dataset, Tadros et al. (2016) identified that the water flow paths to the karst water store may change, as indicated by changes in Sr^{2+} concentrations, and dilution within the karst store was confirmed by decreasing Cl^- concentrations at the end of the Millennium Drought. Changes in the relative volumes of water infiltrating by fast fracture flow and slow fracture flow pathways would be consistent with both the trace element and water isotope monitoring data. The impact of water flow paths in the vadose zone and the differences in $\delta^{18}O$ records between three coeval stalagmites from Harrie Wood Cave is now investigated. Because the relative volumes of water infiltrating by fast fracture flow and slow fracture flow pathways to a storage reservoir varies and each store varies in size and is at a different depth below the surface, it is likely these properties contribute to variability between coeval stalagmite $\delta^{18}O$ values (Treble et al., 2021).

Field evidence shows one major synsedimentary fracture/fault plane coinciding with synsedimentary tectonics and brecciation in the cave ceiling (Fig. 1d in Markowska et al., 2015). The bulk of infiltrating water in the limestone is channelled towards the major synsedimentary fracture, where it is transmitted downwards. Drip site HW1 is located along the fault and HW2 is lateral to the major fracture zone. Field observations indicate that infiltration is through pervasive cracks and fissures (Tadros et al., 2016) and this zone of fissures likely acts as a store for HW1 and HW2, sustaining baseflow, with enhanced drip rates that occur when flow along larger fractures is activated i.e., preferential flow, indicated by the threshold increases in drip rates (Fig. 5). There are fewer cave formations above HW_38 b, indicating less water is stored in this deeper section of the cave and drip logger data from adjacent drip sites display a smaller-magnitude response to infiltration (Markowska et al., 2015).

The observed similarities in HW1 and HW2 hydrochemistry (see Section 3.3) indicate that the common source of water stored in the reservoir is supplied from slow flow drainage, while the difference in the magnitude of the $\delta^{18}O$ response to recharge is interpreted as being related to the contribution of newly recharged water by preferential flow networks (e.g., fissures and fractures) to the reservoir resulting in direct and fast infiltration of the surface signal. The isotopic composition of the drip water, and therefore stalagmite, is related to the isotopic value and volumetric contribution of recharge water to stored water. When the reservoir is at its minimum level, and before seasonal recharge, field evidence indicates drip water $\delta^{18}O$ is from water stored in the karst (Section 3.3). After a major recharge event, the more negative infiltrating $\delta^{18}O$ water mixes with the $\delta^{18}O$ stored water. The net effect is a drop in $\delta^{18}O$ values and the longer monitoring time series for HW-S1 and HW-S2 demonstrate that drip water can shift by 1‰ in response to recharge of the store supporting it (see Section 3.3). However, a higher range in $\delta^{18}O$ values at site HW2 compared to HW1, reflects HW2 drip water is retained in a smaller reservoir than HW1, as a smaller proportion of new recharge water contributes volumetrically to the bulk store water. It is postulated that the most likely explanation for the ~1‰ higher offset in stalagmite HW_38 b from HW-S1 and HW-S2 is due to the smaller reservoir volume supplying drip water to HW_38 b. Hence, the volume of water stored in individual water reservoirs varies and the storage reservoir volume in decreasing order is: HW1, HW2 and HW_38 b. These observations imply that the range of $\delta^{18}O$ values recorded by stalagmites with relatively larger storage reservoirs will be amplified compared with those with smaller reservoirs.

During periods of rainfall deficit, drip water is drained from each storage reservoir to the drip point. The higher discharge at HW1 and HW2 during baseflow conditions, compared to HW_38 b, supports drip water being supplied from a storage reservoir that has a larger volume of water and hydraulic head. The lower discharge observed at HW_38 b supports a connection to a smaller reservoir volume with a relatively small hydraulic head. A smaller store with less connectivity, like HW_38 b, means when the storage reservoir drains there is limited hydrological support to maintain the hydraulic gradient, and this results in a decreased hydraulic head and lower discharge. Also, being located in a deeper part of the cave implies a longer transmission of waters from the storage reservoir to the drip point i.e., a delayed response through the flow paths. The characteristic drip-water geochemical changes at both low and high recharge (see Section 3.3) supports a storage reservoir size which enables the detection of karst processes (e.g., dilution, PCP etc.) through the geochemical variability of the cave drip waters. This interpretation aligns with the existing conceptual model for the dynamic flow regime in Harrie Wood Cave (Fig. 6 in Tadros et al., 2016).

The modelled recharge data for Harrie Wood Cave has shown that recharge is representative of cool season rainfall anomalies at this location (Fig. 6). Cai and Cowan (2008) report a decline of south-eastern Australian autumn rainfall since the early 1990s. Reduced autumn rainfall would delay soil moisture levels from reaching and sustaining field capacity till later in the main (winter) recharge season and therefore reduce the potential for recharge by fracture flow, consistent with the isotopic response documented by Treble et al. (2021). The net effect would be a decrease in karst store recharge during the main winter recharge period and broadly agrees with the timing of the increase in stalagmite $\delta^{18}O$ values during the change in regional hydroclimate between the early to mid-1990's.

Thus, based on field monitoring evidence the dominant influence on variability in stalagmite HW-S1 $\delta^{18}O$ is largely due to a karst recharge response i.e., stores filling and draining in response to recharge, and therefore $\delta^{18}O$ can be used as a recharge proxy for the Australian alpine region of southeast Australia for the last 100 years. This investigation of three $\delta^{18}O$ stalagmite records from Harrie Wood Cave in the Australian Alpine region reveals that Yarrangobilly speleothem $\delta^{18}O$ record recharge variations over the last 84 years. It was also shown that recharge is representative of cool season rainfall anomalies at this location, as well as the broader south-east Australian region, highlighting the suitability of Yarrangobilly speleothem $\delta^{18}O$ for reconstructing past recharge for this important water resource region.

4.2. Comparison with Yarrangobilly Cave and regional records

Quantifying the recharge regime for the period 1920–2006 CE has permitted an understanding of modern stalagmite $\delta^{18}O$ records in the region for the first time. The findings from this research have demonstrated the robustness of using speleothem records to reconstruct past recharge for the Snowy Mountains as well as the broader region. Currently, there are no high-resolution $\delta^{18}O$ speleothem records from the Australian Alps region that overlap chronologically with the modern Harrie Wood Cave records. However, there are two published speleothem records from a nearby cave located within the Yarrangobilly Karst area, Jersey Cave. These records are a $\delta^{18}O$ flowstone record between 99 and 37 ka (YB–F1; Webb et al., 2014) and a 2-ka temperature record reconstructed from stalagmite $\delta^{13}C$ (JC001; McGowan et al., 2018).

The $\delta^{18}O$ record of YB-F1 was suggested to represent rainfall amount (Webb et al., 2014) and that the increase in $\delta^{18}O$ values from 100 to 75 ka reflected reduced rainfall amounts, while the lower flowstone isotopic values from 47 to 37 ka during the wetter warmer interstadial MIS 3 were interpreted to signify larger quantities of rainfall. Corresponding trace element profiles and UV fluorescence were used to support these interpretations. The demonstrated recharge control on stalagmite $\delta^{18}O$ values in this research, rather than a primary rainfall $\delta^{18}O$ signal, has important implications for the interpretation of speleothem isotopic records. In the transition to arid conditions from 100 to 75 ka, Webb et al. (2014) reported $\delta^{18}O$ values between 99 and 84 ka steadily increasing from −6.3 to −2.9‰, and co-varying with $\delta^{13}C$, and alluded to the possibility of kinetic isotope fractionation driving the observed trend (Fig. S1 in Webb et al., 2014). Here we suggest that with extended aridity, increases towards higher values likely reflect limited input to individual storage reservoirs through direct recharge from fast fracture flow (with more negative $\delta^{18}O$ values) and a greater contribution from the slow fracture flow network. Although our key findings still support the interpretation of Webb et al. (2014) i.e., arid conditions from 100 to 75 ka and a wetter interstadial MIS 3, the processes responsible for speleothem isotopic changes is refined here based on new insights into local hydrological processes from our research.

Recently, McGowan et al. (2018) reconstructed a 2000-year annual snow cover record derived from a 104-year linear relationship between the JC001 $\delta^{13}C$ record and local temperature records from the region. In an assessment of global speleothem $\delta^{13}C$ records covering the period between 1900 and 2014 CE, Fohlmeister et al. (2020) also suggests that the dominant control on speleothem $\delta^{13}C$ values are the type of vegetation cover (C3, C4 or CAM plants) and temperature through its influence on soil respiration. In the three modern speleothems in this research, stalagmite $\delta^{13}C$ also decreases when speleothem $\delta^{18}O$ decreases (Supplementary Figure A8) indicating that stalagmite $\delta^{13}C$ is also responding to recharge (Section 3.2). Recharge controls soil-moisture content, which is one of the factors controlling soil respiration processes and therefore the $\delta^{13}C$ composition of soil gas and infiltrating water (Meyer et al., 2014; Fohlmeister et al., 2020). Further, in a global analysis of modern plant and soil $\delta^{13}C$ values, Rao et al. (2017) showed a decrease in soil $\delta^{13}C$ values under C3 vegetation reflected a response to wetter conditions. The Rao et al. (2017) analysis supports the interpretation from this research that increased recharge will lower stalagmite $\delta^{13}C$ values through soil water availability to the C3 dominant vegetation and soil respiration.

The $\delta^{18}O$ record from stalagmite JC001 was not presented by McGowan et al. (2018), as rainfall $\delta^{18}O$ was deemed to be an unreliable proxy for palaeo-hydrology in this region; however, in a different cave system situated 75 km north of Harrie Wood Cave, recent work by Scroxton et al. (2021) shows the potential of a modern stalagmite $\delta^{18}O$ record (CC14-6) from Careys Cave to record multi-year regional droughts. Whilst Careys Cave is in the temperate zone of southeastern Australia, the site experiences higher July mean minimum temperatures ($T_{min} = 3\ ^{\circ}C$) and January mean maximum temperatures ($T_{max} = 29.8\ ^{\circ}C$) by 4.8 °C and 2.2 °C, respectively. Mean annual precipitation is also lower (923 mm yr^{-1}) by 255 mm relative to the Yarrangobilly region, as it is in the rain shadow of the Snowy Mountains region. A response to wet and dry intervals is detectable in the CC14-6 $\delta^{18}O$ record. However, there is a mismatch in the timing of conditions between the CC14-6 record with the three records from Harrie Wood Cave (HW–S1, HW-S2 and HW_38 b). Scroxton et al. (2021) did note a shift of one cycle (ca. 21 years) is plausible in the younger section of CC14-6 due to the uncertainty of whether the stalagmite was active at the time of collection, which could explain the inconsistency between the Careys Cave and Harrie Wood Cave records. Further afield, the upward $\delta^{18}O$ trend from the late 1980s until 1995 CE (Section 3.4) present in the stalagmites from Harrie Wood Cave in this investigation is also similarly observed in a modern stalagmite record from Wellington Cave (Fig. 5d in Markowska et al., 2020). This was similarly interpreted to be due to a decline in recharge impacting the wider south-east Australian region.

Using multi-cave monitoring datasets, it is established that $\delta^{18}O$ values recorded in speleothems from the Australian alpine region do respond to changes in recharge associated with changes in hydroclimate. Evidence presented in this research is a new perspective for the interpretation of $\delta^{18}O$ signals preserved in speleothem records for this region.

4.3. Palaeoclimate implications

This is the first effort to constrain the relationship between climate in the Common Era and $\delta^{18}O$ in a modern speleothem record from an Australian Alpine cave, and one of the few studies worldwide where interpretations are grounded by a long cave-

monitoring dataset from the same site. This research highlights the importance of longer-term cave monitoring data in understanding the links between rainfall $\delta^{18}O$ and drip water $\delta^{18}O$ response to reliably interpret stalagmite $\delta^{18}O$ as a palaeoclimate proxy, and the high value of examining multiple speleothem records within the same cave.

The HW-S1 high-resolution $\delta^{18}O$ time series has been quantitatively assessed and can be regarded as a record of past recharge variability, although the magnitude of the isotopic response to recharge is likely influenced by the volume of karst stores and the antecedent conditions (water levels in the store) at the time of drought or recharge. The Millennium Drought (late 1996 to mid-2010 CE) highlights that longer drought events have more impact on stored karst water. It is anticipated that past intense drought conditions, including the Federation Drought (1895–1903 CE), may be resolved in the stalagmite $\delta^{18}O$ time series from high recharge periods by a shift to high $\delta^{18}O$ values away from the PWM, similar to how $\delta^{18}O$ values were recorded during the Millennium Drought (Fig. 6).

ENSO exerts a major influence on variability in precipitation amount in southeast Australia (Risbey et al., 2009). Theobald and McGowan (2016) found a relationship between ENSO and rainfall in the Australian alpine region over the period 1958–2015, where high (low) precipitation amounts largely coincide with La Niña (El Niño) events. An analysis of climate indices and recharge in this investigation shows a low correlation (Mann-Kendall tests; Section 3.4) and suggests that local geology, land cover and soil type (e.g., soil type, soil moisture availability, antecedent soil moisture conditions) have an additional influence on infiltration and recharge (Barron et al., 2012; Fu et al., 2019). Furthermore, Barron et al. (2012) corroborated the non-linear relationship between rainfall and recharge, with recharge elasticity being between 2 and 4 in Australia, indicating a 10% change in annual rainfall leads to a 20–40% change in recharge. By corollary, the amplification of the drip water, and hence speleothem, $\delta^{18}O$ response to hydroclimate variation via the karst flow paths means that speleothem $\delta^{18}O$ variability cannot be related back to rainfall amount in a linear sense without considering karst flow paths, although could be assisted by adopting a karst forward model (e.g., Baker and Bradley, 2010). In addition, Tadros et al. (2016) inferred that trace element/calcium ratios (e.g., Mg/Ca and Sr/Ca) in the stalagmite will likely be affected by karst hydrological processes in response to changing ENSO phases, where trace element/calcium ratios would shift away from or towards bedrock values during drying and wetting phases. Recent cave monitoring programmes have identified Mg/Ca and Sr/Ca ratios and trace metals as potential geochemical proxies of recharge (e.g., Riechelmann et al., 2022; Wortham et al., 2021). Therefore, consideration of the trace element record over the same growth interval will also assist in the interpretation of past recharge from speleothems in this location.

Furthermore, it should be noted that the modern HW1 drip flow may have been disturbed, evidenced by the unconformity between the paleo-section and the modern growth, whereas HW2 is seemingly less impacted. In HW-S1, the unconformity marks a change in conditions. The palaeo-section is less affected by particulates and has heterotopic shifts due to the shift in the drip point (Fig. 2). This is most likely connected to the 1 m long, 130 mm wide stalactite tip breaking when the main path through the cave was constructed in ~1911 CE (see Table 1 in Tadros et al., 2016). The unconformity can also potentially be related to human activity (e.g., breakage of the stalagmite when the cave was opened and speleothem growth on the broken surface), or alternatively to external conditions. HW-S2 is, however, less modified by potential human intervention and may better represent "pre disturbance" conditions. Thus, comparing the calcite fabrics in the period prior to and following the unconformity will allow for a more complete extrapolation of the modern results to the palaeo-record.

5. Conclusions

Harrie Wood Cave $\delta^{18}O$ stalagmite records can be used as an archive of recharge for the Australian alpine region of southeast Australia. Isotopic fluctuations up to 1.1‰ recorded in the high-resolution HW-S1 $\delta^{18}O$ record is in response to changes in recharge, with speleothem $\delta^{18}O$ values lower than the long-term $\delta^{18}O$ PWM occurring during increased recharge, while reduced recharge causes an increase in $\delta^{18}O$ values close to the $\delta^{18}O$ PWM. Two major droughts in Australia - the World War II Drought (1937–1945 CE) and the Millennium Drought (late 1996 to mid-2010 CE) - were recorded during the 20th and 21st century of speleothem growth (1922–2006 CE) and are expressed as maxima in the stalagmite $\delta^{18}O$ record in response to decreasing recharge. Whilst between 1945 and 1990 CE stalagmite $\delta^{18}O$ values fluctuated in response to changes in recharge, they nonetheless remained below the $\delta^{18}O$ PWM due to more frequent recharging events. This conclusion is supported by 10-years of modern cave monitoring data and an annually constructed recharge timeseries for Harrie Wood Cave. This demonstrates the immense value and important task of long-term monitoring data in guiding the interpretation of speleothem records. The HW-S1 $\delta^{18}O$ record is validated by replication with two other records within the same cave system (HW–S2 and HW_38 b) over the same time interval. The major trends in $\delta^{18}O$ largely replicate, however variation in $\delta^{18}O$ values between the three records is related to karst hydrology, i.e., variability in fracture contribution and the store reservoir volume supplying the drip point.

This is the first modern speleothem $\delta^{18}O$ proxy-climate reconstruction for the Australian Alpine region. The results from this research provide compelling evidence that stalagmites from Harrie Wood Cave, and likely other caves in the Australian alpine region, are sensitive archives of regional recharge. It is anticipated that stalagmite records from the Australian alpine region will now provide direct insights on past variability in recharge. Finally, there is confidence that pre-1900 CE (palaeo) reconstructions based on speleothem $\delta^{18}O$ records from Harrie Wood Cave will show sustained high-recharge years, but also extended drought periods (e.g., the Federation Drought, 1895–1902) which result in long-term variations in regional recharge.

Credit author statement

Carol V. Tadros: Conceptualization, Methodology, Investigation, Formal analysis, Visualization, Writing – original draft, Writing – review & editing. **Monika Markowska:** Investigation, Writing – review & editing. **Pauline C. Treble:** Conceptualization, Investigation, Writing – review & editing. **Andy Baker:** Conceptualization, Methodology, Investigation, Writing – review & editing. **Silvia Frisia:** Investigation, Writing – review & editing. **Lewis Adler:** Investigation, Writing – review & editing. **Russell N. Drysdale:** Investigation, Writing – review & editing.

Declaration of competing interest

The authors declare that they have no known competing financial interests or personal relationships that could have appeared to influence the work reported in this paper.

Data availability

Data will be made available on request.

Acknowledgements

We highly appreciate the editorial work of AE Miryam Bar-Matthews and thank A. Ayalon and two anonymous reviewers for their contribution to the peer review of this work. The authors thank the NSW NPWS Yarrangobilly Caves manager and staff for their on-going collection of rainfall and drip water samples, Barbora Gallagher and Jennifer van Holst for their assistance in water isotope analyses and Stuart Hankin for assistance in generating Fig. 1.

Appendix A. Supplementary data

Supplementary data to this article can be found online at https://doi.org/10.1016/j.quascirev.2022.107742.

References

Aplin, K., Ford, F.D., Hiscock, P., 2010. Early Holocene human occupation and environment of the southeast Australian Alps: new evidence from the yarrangobilly plateau, New South Wales. In: Altered Ecologies: Fire, Climate and Human Influence on Terrestrial Landscapes (Terra Australis 32). ANU ePress.
Baker, A., Bradley, C., 2010. Modern stalagmite δ18O: instrumental calibration and forward modelling. Global Planet. Change 71 (3–4), 201–206.
Baker, A., Hartmann, A., Duan, W., Hankin, S., Comas-Bru, L., Cuthbert, M.O., Treble, P.C., Banner, J., Genty, D., Baldini, L.M., Bartolomé, M., 2019. Global analysis reveals climatic controls on the oxygen isotope composition of cave drip water. Nat. Commun. 10 (1), 1–7.
Baker, A., Scheller, M., Oriani, F., Mariethoz, G., Hartmann, A., Wang, Z., Cuthbert, M.O., 2021. Quantifying temporal variability and spatial heterogeneity in rainfall recharge thresholds in a montane karst environment. J. Hydrol. 594, 125965.
Barron, O.V., Crosbie, R.S., Dawes, W.R., Charles, S.P., Pickett, T., Donn, M.J., 2012. Climatic controls on diffuse groundwater recharge across Australia. Hydrol. Earth Syst. Sci. 16 (12), 4557–4570.
BoM, 2022. http://www.bom.gov.au/climate/data/. (Accessed 16 May 2022).
Cai, W., Cowan, T., 2008. Evidence of impacts from rising temperature on inflows to the Murray-Darling Basin. Geophys. Res. Lett. 35 (7).
Chiarini, V., Couchoud, I., Drysdale, R., Bajo, P., Milanolo, S., Frisia, S., Greig, A., Hellstrom, J., De Waele, J., 2017. Petrographical and geochemical changes in Bosnian stalagmites and their palaeo-environmental significance. Int. J. Speleol. 46 (1), 33–49.
Coleborn, K., Baker, A., Treble, P.C., Andersen, M.S., Baker, A., Tadros, C.V., Tozer, M., Fairchild, I.J., Spate, A., Meehan, S., 2018. The impact of fire on the geochemistry of speleothem-forming drip water in a sub-alpine cave. Sci. Total Environ. 642, 408–420.
Coleborn, K., Baker, A., Treble, P.C., Andersen, M.S., Baker, A., Tadros, C.V., Tozer, M., Fairchild, I.J., Spate, A., Meehan, S., 2019. Corrigendum to" the impact of fire on the geochemistry of speleothem-forming drip water in a sub-alpine cave"[Sci. Total Environ.(2018) 408-420]. Sci. Total Environ. 668, 1339–1340.
Collister, C., Mattey, D., 2008. Controls on water drop volume at speleothem drip sites: an experimental study. J. Hydrol. 358 (3–4), 259–267.
Coplen, T.B., 1988. Normalization of oxygen and hydrogen isotope data. Chem. Geol. Isot. Geosci. 72 (4), 293–297.
Coplen, T.B., 2007. Calibration of the calcite–water oxygen-isotope geothermometer at Devils Hole, Nevada, a natural laboratory. Geochem. Cosmochim. Acta 71 (16), 3948–3957.
Cruz Jr., F.W., Karmann, I., Viana Jr., O., Burns, S.J., Ferrari, J.A., Vuille, M., Sial, A.N., Moreira, M.Z., 2005. Stable isotope study of cave percolation waters in subtropical Brazil: implications for paleoclimate inferences from speleothems. Chem. Geol. 220 (3–4), 245–262.
Dansgaard, W., 1964. Stable isotopes in precipitation. Tellus 16 (4), 436–468.
Deininger, M., Scholz, D., 2019. Isolution 1.0: an ISOtope evoLUTION model describing the stable oxygen (δ 18 O) and carbon (δ 13 C) isotope values of speleothems. Int. J. Speleol. 48 (1), 21–32.
Deininger, M., Hansen, M., Fohlmeister, J., Schröder-Ritzrau, A., Burstyn, Y., Scholz, D., 2021. Are oxygen isotope fractionation factors between calcite and water derived from speleothems systematically biased due to prior calcite precipitation (PCP)? Geochem. Cosmochim. Acta 305, 212–227.
Dixon, B.C., Tyler, J.J., Lorrey, A.M., Goodwin, I.D., Gergis, J., Drysdale, R.N., 2017. Low-resolution Australasian palaeoclimate records of the last 2000 years. Clim. Past 13 (10), 1403–1433.
Fairchild, I.J., Baker, A., 2012. Speleothem Science: from Process to Past Environments. John Wiley & Sons.
Feng, W., Banner, J.L., Guilfoyle, A.L., Musgrove, M., James, E.W., 2012. Oxygen isotopic fractionation between drip water and speleothem calcite: a 10-year monitoring study, central Texas, USA. Chem. Geol. 304, 53–67.
Fohlmeister, J., Voarintsoa, N.R.G., Lechleitner, F.A., Boyd, M., Brandtstätter, S., Jacobson, M.J., Oster, J., 2020. Main controls on the stable carbon isotope composition of speleothems. Geochem. Cosmochim. Acta 279, 67–87.
Freund, M., Henley, B.J., Karoly, D.J., Allen, K.J., Baker, P.J., 2017. Multi-century cool- and warm-season rainfall reconstructions for Australia's major climatic regions. Clim. Past 13 (12), 1751–1770.
Frisia, S., 2015. Microstratigraphic logging of calcite fabrics in speleothems as tool for palaeoclimate studies. Int. J. Speleol. 44 (1), 1–16.
Frisia, S., Borsato, A., Hellstrom, J., 2018. High spatial resolution investigation of nucleation, growth and early diagenesis in speleothems as exemplar for sedimentary carbonates. Earth Sci. Rev. 178, 68–91.
Fu, G., Crosbie, R.S., Barron, O., Charles, S.P., Dawes, W., Shi, X., Van Niel, T., Li, C., 2019. Attributing variations of temporal and spatial groundwater recharge: a statistical analysis of climatic and non-climatic factors. J. Hydrol. 568, 816–834.
Gat, J.R., 1996. Oxygen and hydrogen isotopes in the hydrologic cycle. Annu. Rev. Earth Planet Sci. 24 (1), 225–262.
Genty, D., Labuhn, I., Hoffmann, G., Danis, P.A., Mestre, O., Bourges, F., Wainer, K., Massault, M., Van Exter, S., Régnier, E., Orengo, P., 2014. Rainfall and cave water isotopic relationships in two South-France sites. Geochem. Cosmochim. Acta 131, 323–343.
Green, K., Pickering, C.M., 2009. The decline of snowpatches in the Snowy Mountains of Australia: importance of climate warming, variable snow, and wind. Arctic Antarct. Alpine Res. 41 (2), 212–218.
Hennessy, K., Whetton, P., Smith, I., Bathols, J., Hutchinson, M., Sharples, J., 2003. The Impact of Climate Change on Snow Conditions in Mainland Australia. CSIRO, Aspendale.
Hercman, H., Gąsiorowski, M., Pawlak, J., Błaszczyk, M., Gradziński, M., Matoušková, Š., Zawidzki, P., Bella, P., 2020. Atmospheric circulation and the differentiation of precipitation sources during the Holocene inferred from five stalagmite records from Demänová Cave System (Central Europe). The Holocene 30 (6), 834–846.
Jex, C.N., Baker, A., Fairchild, I.J., Eastwood, W.J., Leng, M.J., Sloane, H.J., Thomas, L., Bekaroğlu, E., 2010. Calibration of speleothem δ18O with instrumental climate records from Turkey. Global Planet. Change 71 (3–4), 207–217.
Johnston, V.E., Borsato, A., Spötl, C., Frisia, S., Miorandi, R., 2013. Stable isotopes in caves over altitudinal gradients: fractionation behaviour and inferences for speleothem sensitivity to climate change. Clim. Past 9 (1), 99–118.
Kim, S.T., O'Neil, J.R., 1997. Equilibrium and nonequilibrium oxygen isotope effects in synthetic carbonates. Geochem. Cosmochim. Acta 61 (16), 3461–3475.
Lachniet, M.S., 2009. Climatic and environmental controls on speleothem oxygen-isotope values. Quat. Sci. Rev. 28 (5–6), 412–432.
Markowska, M., 2012. Characterising Drip Water Hydrology of the Karst Unsaturated Zone in Harrie Wood Cave, Yarrangobilly. Honours Thesis. UNSW, Sydney, Kensington, Australia.
Markowska, M., Baker, A., Treble, P.C., Andersen, M.S., Hankin, S., Jex, C.N., Tadros, C.V., Roach, R., 2015. Unsaturated zone hydrology and cave drip discharge water response: implications for speleothem paleoclimate record variability. J. Hydrol. 529, 662–675.
Markowska, M., Fohlmeister, J., Treble, P.C., Baker, A., Andersen, M.S., Hua, Q., 2019. Modelling the 14C bomb-pulse in young speleothems using a soil carbon continuum model. Geochem. Cosmochim. Acta 261, 342–367.
Markowska, M., Cuthbert, M.O., Baker, A., Treble, P.C., Andersen, M.S., Adler, L., Griffiths, A., Frisia, S., 2020. Modern speleothem oxygen isotope hydroclimate records in water-limited SE Australia. Geochem. Cosmochim. Acta 270, 431–448.
Mattey, D., Lowry, D., Duffet, J., Fisher, R., Hodge, E., Frisia, S., 2008. A 53 year seasonally resolved oxygen and carbon isotope record from a modern Gibraltar speleothem: reconstructed drip water and relationship to local precipitation. Earth Planet Sci. Lett. 269 (1–2), 80–95.
McDermott, F., 2004. Palaeo-climate reconstruction from stable isotope variations in speleothems: a review. Quat. Sci. Rev. 23 (7–8), 901–918.
McGowan, H., Callow, J.N., Soderholm, J., McGrath, G., Campbell, M., Zhao, J.X., 2018. Global warming in the context of 2000 years of Australian alpine temperature and snow cover. Sci. Rep. 8 (1), 1–8.
Meyer, K.W., Feng, W., Breecker, D.O., Banner, J.L., Guilfoyle, A., 2014. Interpretation of speleothem calcite δ13C variations: evidence from monitoring soil CO2, drip water, and modern speleothem calcite in central Texas. Geochem. Cosmochim. Acta 142, 281–298.
Mickler, P.J., Banner, J.L., Stern, L., Asmerom, Y., Edwards, R.L., Ito, E., 2004. Stable isotope variations in modern tropical speleothems: evaluating equilibrium vs. kinetic isotope effects. Geochem. Cosmochim. Acta 68 (21), 4381–4393.
Moquet, J.S., Cruz, F.W., Novello, V.F., Stríkis, N.M., Deininger, M., Karmann, I., Santos, R.V., Millo, C., Apaestegui, J., Guyot, J.L., Siffedine, A., 2016. Calibration of speleothem δ18O records against hydroclimate instrumental records in Central Brazil. Global Planet. Change 139, 151–164.
Neukom, R., Gergis, J., 2012. Southern Hemisphere high-resolution palaeoclimate records of the last 2000 years. Holocene 22 (5), 501–524.
Nicholl, O., 1974. Harrie Wood Cave Map–Y26. Yarrangobilly Research Group and Canberra Speleological Society, Canberra.
Rao, Z., Guo, W., Cao, J., Shi, F., Jiang, H., Li, C., 2017. Relationship between the stable carbon isotopic composition of modern plants and surface soils and climate: a global review. Earth Sci. Rev. 165, 110–119.
Rauniyar, S.P., Power, S.B., 2020. The impact of anthropogenic forcing and natural processes on past, present, and future rainfall over Victoria, Australia. J. Clim. 33 (18), 8087–8106.
Riechelmann, S., Schröder-Ritzrau, A., Spötl, C., Riechelmann, D.F.C., Richter, D.K., Mangini, A., Frank, N., Breitenbach, S.F., Immenhauser, A., 2017. Sensitivity of

Bunker Cave to climatic forcings highlighted through multi-annual monitoring of rain-, soil-, and dripwaters. Chem. Geol. 449, 194–205.
Riechelmann, D.F.C., Riechelmann, S., Schröder-Ritzrau, A., 2022. Long-term elemental trends in drip waters from monitoring Bunker Cave: new insights for past precipitation variability. Chem. Geol. 590, 120704.
Risbey, J.S., Pook, M.J., McIntosh, P.C., Wheeler, M.C., Hendon, H.H., 2009. On the remote drivers of rainfall variability in Australia. Mon. Weather Rev. 137 (10), 3233–3253.
Rozanski, K., Araguás-Araguás, L., Gonfiantini, R., 1993. Isotopic patterns in modern global precipitation. Climate change in continental isotopic records 78, 1–36.
Scroxton, N., Walczak, M., Markowska, M., Zhao, J.X., Fallon, S., 2021. Historical droughts in Southeast Australia recorded in a New South Wales stalagmite. The Holocene 31 (4), 607–617.
Tadros, C.V., Treble, P.C., Baker, A., Fairchild, I., Hankin, S., Roach, R., Markowska, M., McDonald, J., 2016. ENSO-cave drip water hydrochemical relationship: a 7-year dataset from south-eastern Australia. Hydrol. Earth Syst. Sci. 20 (11), 4625–4640.
Tadros, C.V., Treble, P.C., Baker, A., Hankin, S., Roach, R., 2019. Cave drip water solutes in south-eastern Australia: constraining sources, sinks and processes. Sci. Total Environ. 651, 2175–2186.
Tan, M., 2014. Circulation effect: response of precipitation δ18O to the ENSO cycle in monsoon regions of China. Clim. Dynam. 42 (3), 1067–1077.
Theobald, A., McGowan, H., 2016. Evidence of increased tropical moisture in southeast Australian alpine precipitation during ENSO. Geophys. Res. Lett. 43 (20), 10,901–10,908.
Treble, P., Baker, A., Hellstrom, J.C., Abram, N., Crawford, J., Gagan, M., Borsato, A., Griffiths, A., Bajo, P., Markowska, M., Priestley, S., 2021. Quantification of the Hydrological Control on Speleothem Oxygen Isotopic Variability.
Tremaine, D.M., Froelich, P.N., Wang, Y., 2011. Speleothem calcite farmed in situ: modern calibration of δ18O and δ13C paleoclimate proxies in a continuously-monitored natural cave system. Geochem. Cosmochim. Acta 75 (17), 4929–4950.
Wang, X., Edwards, R.L., Auler, A.S., Cheng, H., Kong, X., Wang, Y., Cruz, F.W., Dorale, J.A., Chiang, H.W., 2017. Hydroclimate changes across the Amazon lowlands over the past 45,000 years. Nature 541 (7636), 204–207.
Webb, M., Dredge, J., Barker, P.A., Müller, W., Jex, C., Desmarchelier, J., Hellstrom, J., Wynn, P.M., 2014. Quaternary climatic instability in south-east Australia from a multi-proxy speleothem record. J. Quat. Sci. 29 (6), 589–596.
Worboys, G.L., Good, R.B., 2011. Caring for Our Australian Alps Catchments: Summary Report for Policy Makers. Department of Climate Change and Energy Efficiency, Canberra.
Wortham, B.E., Montañez, I.P., Bowman, K., Kuta, D., Soto Contreras, N., Brummage, E., Pang, A., Tinsley, J., Roemer-Baer, G., 2021. Monitoring of Sierra Nevada caves reveals the potential for stalagmites to archive seasonal variability. Front. Earth Sci. 1319. https://doi.org/10.3389/feart.2021.781526, 781526.
Zhang, J., Genty, D., Sirieix, C., Michel, S., Minster, B., Régnier, E., 2020. Quantitative assessments of moisture sources and temperature governing rainfall δ18O from 20 years' monitoring records in SW-France: importance for isotopic-based climate reconstructions. J. Hydrol. 591, 125327.